Received: 26 October 2022 | Accepted: 1 February 2023

DOI: 10.1111/gcb.16755

Global Change Biology WILEY

RESEARCH ARTICLE

Observational constraints reduce model spread but not uncertainty in global wetland methane emission estimates

Kuang-Yu Chang[1] | William J. Riley[1] | Nathan Collier[2] | Gavin McNicol[3] | Etienne Fluet-Chouinard[4] | Sara H. Knox[5] | Kyle B. Delwiche[6] | Robert B. Jackson[7,8,9] | Benjamin Poulter[10] | Marielle Saunois[11] | Naveen Chandra[12] | Nicola Gedney[13] | Misa Ishizawa[14] | Akihiko Ito[15] | Fortunat Joos[16,17] | Thomas Kleinen[18] | Federico Maggi[19] | Joe McNorton[20] | Joe R. Melton[21] | Paul Miller[22,23] | Yosuke Niwa[15,24] | Chiara Pasut[19,25] | Prabir K. Patra[26,27] | Changhui Peng[28,29] | Sushi Peng[30] | Arjo Segers[31] | Hanqin Tian[32] | Aki Tsuruta[33] | Yuanzhi Yao[34] | Yi Yin[35] | Wenxin Zhang[22] | Zhen Zhang[36,37] | Qing Zhu[1] | Qiuan Zhu[38] | Qianlai Zhuang[39]

[1]Climate and Ecosystem Sciences Division, Lawrence Berkeley National Laboratory, Berkeley, California, USA
[2]Climate Change Science Institute, Oak Ridge National Laboratory, Oak Ridge, Tennessee, USA
[3]Department of Earth and Environmental Sciences, University of Illinois Chicago, Chicago, Illinois, USA
[4]Institute for Atmospheric and Climate Science, ETH Zurich, Zurich, Switzerland
[5]Department of Geography, The University of British Columbia, Vancouver, British Columbia, Canada
[6]Department of Environmental Science, Policy & Management, UC Berkeley, Berkeley, California, USA
[7]Department of Earth System Science, Stanford University, Stanford, California, USA
[8]Woods Institute for the Environment, Stanford University, Stanford, California, USA
[9]Precourt Institute for Energy, Stanford University, Stanford, California, USA
[10]Biospheric Sciences Laboratory, NASA Goddard Space Flight Center, Greenbelt, Maryland, USA
[11]Laboratoire des Sciences du Climat et de l'Environnement, LSCE-IPSL (CEA-CNRS-UVSQ), Université Paris-Saclay, Gif-sur-Yvette, France
[12]Institute of Arctic Climate and Environment Research (IACE), JAMSTEC, Yokohama, Japan
[13]Met Office Hadley Centre, Joint Centre for Hydrometeorological Research, Wallingford, UK
[14]Climate Research Division, Environment and Climate Change Canada, Toronto, Ontario, Canada
[15]Earth System Division, National Institute for Environmental Studies (NIES), Tsukuba, Japan
[16]Climate and Environmental Physics, University of Bern, Bern, Switzerland
[17]Oeschger Centre for Climate Change Research, University of Bern, Bern, Switzerland
[18]Max Planck Institute for Meteorology, Hamburg, Germany
[19]School of Civil Engineering, The University of Sydney, Sydney, Australia
[20]Research Department, European Centre for Medium-Range Weather Forecasts, Reading, UK
[21]Climate Research Division, Environment and Climate Change Canada, Victoria, British Columbia, Canada
[22]Department of Physical Geography and Ecosystem Science, Lund University, Lund, Sweden
[23]Centre for Environmental and Climate Science, Lund University, Lund, Sweden
[24]Meteorological Research Institute (MRI), Tsukuba, Japan
[25]CSIRO Agriculture & Food, Urrbrae, South Australia, Australia
[26]Research Institute for Global Change, JAMSTEC, Yokohama, Japan
[27]Center for Environmental Remote Sensing, Chiba University, Chiba, Japan
[28]College of Resources and Environmental Science, Hunan Normal University, Changsha, China
[29]Department of Biology Sciences, University of Québec at Montreal, Montreal, Québec, Canada
[30]Sino-French Institute for Earth System Science, College of Urban and Environmental Sciences, Peking University, Beijing, China

[31]Netherlands Organisation for Applied Scientific Research (TNO), Utrecht, The Netherlands
[32]Department of Earth and Environmental Sciences, Schiller Institute for Integrated Science and Society, Boston College, Chestnut Hill, Massachusetts, USA
[33]Finnish Meteorological Institute, Helsinki, Finland
[34]School of Geographic Sciences, East China Normal University, Shanghai, China
[35]Division of Geophysical and Planetary Science, California Institute of Technology, Pasadena, California, USA
[36]Earth System Science Interdisciplinary Center, University of Maryland, College Park, Maryland, USA
[37]Institute of Tibetan Plateau Research, Chinese Academy of Sciences, Beijing, China
[38]College of Hydrology and Water Resources, Hohai University, Nanjing, China
[39]Department of Earth, Atmospheric, and Planetary Sciences, Department of Agronomy, Purdue University, Indiana, West Lafayette, USA

Correspondence
Kuang-Yu Chang, Climate and Ecosystem Sciences Division, Lawrence Berkeley National Laboratory, Berkeley, CA 94720, USA.
Email: ckychang@lbl.gov

Funding information
U.S. Department of Energy Office of Science, Grant/Award Number: DE-AC02-05CH11231; Gordon and Betty Moore Foundation, Grant/Award Number: GBMF5439; Swiss National Science Foundation, Grant/Award Number: 200020_200511; National Computational Infrastructure of the Australian Government, Grant/Award Number: NCMAS-2021-78; Met Office Climate Science for Service Partnership Brazil (CSSP Brazil)

Abstract

The recent rise in atmospheric methane (CH_4) concentrations accelerates climate change and offsets mitigation efforts. Although wetlands are the largest natural CH_4 source, estimates of global wetland CH_4 emissions vary widely among approaches taken by bottom-up (BU) process-based biogeochemical models and top-down (TD) atmospheric inversion methods. Here, we integrate in situ measurements, multi-model ensembles, and a machine learning upscaling product into the International Land Model Benchmarking system to examine the relationship between wetland CH_4 emission estimates and model performance. We find that using better-performing models identified by observational constraints reduces the spread of wetland CH_4 emission estimates by 62% and 39% for BU- and TD-based approaches, respectively. However, global BU and TD CH_4 emission estimate discrepancies increased by about 15% (from 31 to 36 $TgCH_4$ $year^{-1}$) when the top 20% models were used, although we consider this result moderately uncertain given the unevenly distributed global observations. Our analyses demonstrate that model performance ranking is subject to benchmark selection due to large inter-site variability, highlighting the importance of expanding coverage of benchmark sites to diverse environmental conditions. We encourage future development of wetland CH_4 models to move beyond static benchmarking and focus on evaluating site-specific and ecosystem-specific variabilities inferred from observations.

KEYWORDS
benchmarking, bottom-up models, eddy covariance, methane emissions, observational constraints, top-down models, wetland modeling

1 | INTRODUCTION

Methane (CH_4) is the second most important heat trapping gas after carbon dioxide (Saunois et al., 2020; Stavert et al., 2022) and was responsible for ~0.5°C of anthropogenic global warming in the 2010s relative to the late 19th century (IPCC, 2021). Understanding and quantifying the global CH_4 budget is important for climate mitigation due to the relatively short atmospheric lifetime (12.4 years, Balcombe et al. (2018)) and strong radiative forcing (Allen et al., 2018; Neubauer & Patrick Megonigal, 2015) of CH_4. The global mean CH_4 concentration in the atmosphere has increased from about 1775 parts per billion (ppb) in 2016 to 1890 ppb in 2020, more than two-and-a-half times preindustrial levels (Jackson et al., 2020; Lan et al., 2023; Nisbet et al., 2019). The annual growth rate of atmospheric CH_4 estimated in 2021 was a record high since 1984 (18.05 ± 0.38 ppb $year^{-1}$, Lan et al., 2023), and almost three times higher than the average annual growth rate of 6.4 ppb $year^{-1}$ during 2007 to 2015 (Poulter et al., 2017). Importantly, global CH_4 concentrations have continued to rise over the past decade, consistently with the SSP5-8.5 projections (Shared Socioeconomic Pathways) which yield a radiative forcing of 8.5 W m^{-2} in 2100 (Saunois, Jackson, et al., 2016; Saunois et al., 2020). The soaring atmospheric CH_4 concentration in 2020 is likely attributed to the warmer and wetter conditions over wetlands with decreased tropospheric concentration of the hydroxyl radical

(OH, which is the main sink of atmospheric CH_4 concentration; Peng et al., 2022).

With regards to the global CH_4 budget, bottom-up (BU)- and top-down (TD)-based global CH_4 emission estimates both increased from 2000–2009 to 2008–2017 (BU: 547 (524–560) to 576 (550–594) $TgCH_4$ $year^{-1}$; TD: 703 (566–842) to 737 (594–881) $TgCH_4$ $year^{-1}$), and the mismatch between BU and TD estimates has remained large over the past decades (Kirschke et al., 2013; Saunois et al., 2020; Saunois, Bousquet, et al., 2016). For natural wetland CH_4 emissions, the BU estimates rely on process-based biogeochemical models that parameterize CH_4 production and emission rates, and the TD estimates are based on atmospheric inverse modeling that do not present CH_4 production processes. The discrepancies between global CH_4 emission estimates inferred from BU and TD approaches are most likely driven by double counting CH_4 emission sources and extrapolating local measurements (Stavert et al., 2022). Such discrepancies make it difficult to accurately quantify the global CH_4 budget and obscure the estimated global warming potential attributed to changes in atmospheric CH_4 concentrations. Wetlands, which account for the largest CH_4 emissions in the global budget (20%–31% of global CH_4 emissions), also have the largest absolute and relative differences between TD and BU estimates (about 32 $TgCH_4$ $year^{-1}$, TD minus BU), even with recent advances in CH_4 observations and simulations (Saunois et al., 2020).

Accurate wetland CH_4 emission estimates are hindered by high spatial and temporal variability associated with coupled hydrological, biological, and climatic drivers at the site-level scale (Chang et al., 2019; Grant et al., 2019; Hemes et al., 2018; Morin et al., 2017), and upscaling patchy measurements and wetland areal extent at the global scale (Melton et al., 2013; Poulter et al., 2017; Zhang et al., 2021). Insufficient global representation of CH_4 observations and incomplete understanding of CH_4 production, oxidation, and transport processes limit the ability to evaluate and improve global wetland CH_4 emission estimates. Currently, the model spread of wetland CH_4 emission within estimation approaches (BU: 80 $TgCH_4$ $year^{-1}$; TD: 41 $TgCH_4$ $year^{-1}$) is comparable to the discrepancy between ensemble BU and TD approaches (32 $TgCH_4$ $year^{-1}$, TD minus BU; Saunois et al., 2020), complicating the interpretation of different BU and TD CH_4 emission estimates.

Both BU and TD approaches are faced with several challenges to improve their estimates of wetland CH_4 emissions. Issues known to be important for BU wetland CH_4 emission estimates include (1) incomplete process representation of CH_4 biogeochemistry, (2) substantial structural and parameter uncertainty in biogeochemical models, and (3) insufficient measurements to evaluate model performance (Bohn et al., 2015; Chadburn et al., 2020; Chang et al., 2020; Melton et al., 2013; Riley et al., 2011; Wania et al., 2013). TD wetland CH_4 emission estimates are sensitive to uncertainties in (1) CH_4 concentration data used in the inversion framework, (2) atmospheric chemistry and transport, and (3) prior emission estimates (Houweling et al., 2017; Inoue et al., 2016; Maasakkers et al., 2021). Wetland CH_4 model intercomparison projects were conducted to assess the predictability of wetland CH_4 emissions and areas, aiming to reduce emission uncertainties and guide future CH_4 model development. For example, the intercomparison of wetland CH_4 emissions models over West Siberia (WETCHIMP-WSL) found that CH_4 model performance is primarily affected by the reliability of soil thermal and hydrological representations instead of the underlying biogeochemical schemes (Bohn et al., 2015). More recently, a study has demonstrated the potential of imposing satellite-informed CH_4 emission constraints to refine BU wetland CH_4 emission estimates, although the emission range inferred from the highest-performance BU models remains wide (117–189 $TgCH_4$ $year^{-1}$; Ma et al., 2021).

Global compilations of in situ flux measurements could provide key observational constraints for wetland CH_4 biogeochemistry (Delwiche et al., 2021; Knox et al., 2019). The recently released FLUXNET-CH_4 community product includes eddy covariance CH_4 flux measurements across multiple wetland ecosystem types. These site-level measurements have been applied to demonstrate environmental controls on emergent CH_4 dynamics across diurnal to seasonal timescales (Chang et al., 2021; Knox et al., 2021) that help guide process-based biogeochemical model development. Yet, the FLUXNET-CH_4 measurements have not been leveraged to thoroughly benchmark BU and TD models and their estimates of global CH_4 emissions.

Here, we use a model down-selection approach, based on constraints inferred from observations and simulations, to evaluate whether BU and TD wetland CH_4 emission estimates can be reconciled with model performance ranking. Specifically, we evaluate whether the modeled global wetland CH_4 emissions converge into the common range estimated by BU- and TD-based approaches (159–182 $TgCH_4$ $year^{-1}$) with better-performing models identified with the FLUXNET-CH_4 measurements. We test the hypothesis that filtering based on model performance reduces wetland CH_4 emission prediction range and uncertainty. We also used machine learning-based global wetland CH_4 emission estimates to evaluate model benchmarking sensitivity to constraints inferred from different geographical regions. BU and TD models are compared to reference datasets at two geographic scales: at sites from an observational network, and at the global scale covering the entire world land area. In this way, we explore ways to refine ensemble global wetland CH_4 emission estimates, acknowledging the limitations in currently available reference datasets. Model benchmarking metrics calculated by the International Land Model Benchmarking (ILAMB) system (Collier et al., 2018) are used to assess model performance across ecosystem and global scales.

2 | METHODS AND DATA

2.1 | FLUXNET-CH_4 community product

The FLUXNET-CH_4 community product was initiated by the Global Carbon Project in coordination with regional flux networks, including AmeriFlux, the European Fluxes Database, and the Integrated Carbon Observation System Ecosystem Thematic Centre

(ICOS-ETC), to better constrain global CH_4 emission estimates. The database compiled eddy covariance and supporting measurements from 81 sites (including 42 freshwater wetlands, 6 coastal wetlands, and 7 rice paddies) encompassing boreal, temperate, subtropical, and tropical regions. Database descriptions, including site characteristics, data standardization, gap-filling, and partitioning, have been detailed previously in Delwiche et al. (2021) and Knox et al. (2019).

In this study, we used daily mean air temperature, precipitation, and CH_4 emissions compiled at the 42 freshwater wetland sites (Table S1) available in the FLUXNET-CH_4 database (CC-BY-4.0), comprising 169 site-years spanning from 2006 to 2018 (Figure S1). To evaluate monthly model predictions (Sections 2.2 and 2.3), we aggregated daily CH_4 flux measurements gap-filled using the artificial neural network (ANN) method described in Delwiche et al. (2021; FCH4_F_ANN_mean) to the monthly resolution of most BU and TD models.

We note here that the measurement uncertainties associated with the high temporal variability (Hemes et al., 2018) and large spatial heterogeneity (Rey-Sanchez et al., 2022) of wetland CH_4 emissions could affect the interpretation of model-data benchmarking results. For example, the scale mismatch between eddy covariance flux footprints (~0.001 to 10 km^2; Chu et al., 2021) and global wetland CH_4 models (~100 km^2) challenges the robustness of model performance evaluation. Using gap-filled data to enhance the spatial and temporal data coverage for model-data benchmarking could also introduce noises to the true observational signals, although such uncertainties can be quantified and reduced Delwiche et al. (2021). While the accuracy of eddy covariance measurements is limited by measurement uncertainties, site-level measurements are currently the only observational constraints on emission patterns across diel to annual timescales that provide benchmarks for the temporal dynamics represented in wetland CH_4 models.

2.2 | Bottom-up biogeochemical models

In this work, we collected global simulations of wetland CH_4 emission estimates from 14 process-based biogeochemical models (Table S2; Figure S2). BU models were run under a common protocol described in Saunois et al. (2020), driven by climate forcing provided by CRU-JRA reanalysis data (Harris, 2019) from 1901 to 2017. For our site-level analyses, we evaluate the modeled CH_4 emission density per wetland area against observed wetland CH_4 emissions. For our global-scale analyses, gridded CH_4 emission density estimates ($mgCH_4\ m^{-2}\ day^{-1}$, for each gridcell area) were weighted by the Wetland Area and Dynamics for Methane Modeling (WAD2M) wetland area and dynamics dataset (wetland area per gridcell area; Zhang et al., 2021) to prescribe consistent wetland area dynamics across models.

2.3 | Top-down atmospheric inversion models

TD atmospheric inversion models calculate surface-to-atmosphere fluxes by linking atmospheric trace gas observations, an atmospheric chemistry transport model, and prior constraints on the flux estimates (Houweling et al., 2017). The 22 inversion runs (Table S3; Figure S2) of gridded CH_4 emission estimates reported in the latest global CH_4 budget (2000–2017; Saunois et al., 2020) were used in this evaluation. These 22 TD estimates are based on nine atmospheric inversion systems using global Eulerian transport models (Saunois et al., 2020). Each inversion system provided one, two, or four gridded CH_4 emission estimates for the period 2000–2017, driven by different atmospheric CH_4 observations (surface measurements and/or satellite retrievals) and prior emission distributions. Gridded CH_4 emission estimates were further designated into five source categories: wetlands, natural non-wetland sources, agriculture and waste, biomass burning and biofuels, and fossil fuel. Gridded wetland CH_4 emission estimates were obtained from (1) optimized posterior fluxes if an inversion had solved CH_4 emissions per source category, or (2) prior contribution of fluxes scaled by the ratio of total posterior emissions to total prior emissions if an inversion only solved for total emissions (or for categories other than the five categories described above; Kirschke et al., 2013; Saunois et al., 2020).

The prior constraints on wetland CH_4 emission estimates used in each TD inversion system are summarized in Table S3, and detailed descriptions of the 22 inversion runs can be found in Saunois et al. (2020). At the site scale, we used FLUXNET-CH_4 measurements to evaluate wetland CH_4 emissions inferred from individual TD inversion estimates, assuming eddy covariance observations represent gridcell wetland biogeochemistry. For the global-scale analysis, the wetland CH_4 emission density per gridcell area outputted by TD models was weighted by the WAD2M wetland area and dynamics dataset (Zhang et al., 2021) to evaluate TD-based CH_4 emission density per wetland area against other datasets.

2.4 | Machine learning-based global wetland CH_4 emission upscaling

Machine learning (ML) techniques have been used to extrapolate ecosystem-scale wetland CH_4 measurements into global-scale wetland CH_4 emission distributions. In this study, we draw from a recently developed machine learning global wetland CH_4 emissions dataset (UPCH_4 dataset; McNicol et al., Submitted) inferred from eddy covariance measurements collected at 43 freshwater wetland sites across the globe. The locations of the 43 freshwater wetland sites are presented in Figure 1f, encompassing the 42 freshwater wetland sites used in this study and the Scotty Creek Landscape (CA-SCC) in Canada that was not categorized as freshwater wetland in Delwiche et al. (2021). The UPCH_4 dataset reports annual global wetland CH_4 emission estimates of 146 ± 43 $TgCH_4\ year^{-1}$ for 2001–2018, which is within the range of values inferred from the latest BU and TD estimates reported in (Saunois et al., 2020). The UPCH_4 dataset was generated by training a random-forest model with predictors from climatic variables (e.g., air temperature), biometeorological variables

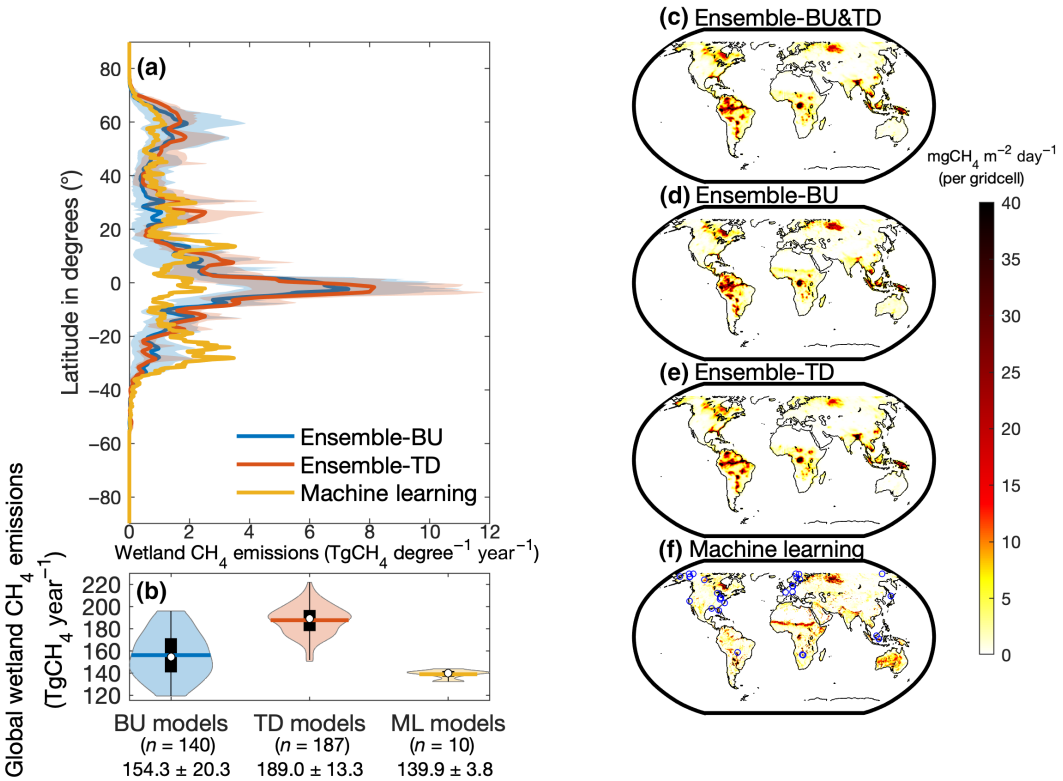

FIGURE 1 Global wetland CH_4 emission estimates inferred from bottom-up (BU) biogeochemical models, top-down (TD) atmospheric inversion models, and a machine learning model ($UPCH_4$; ML). The latitudinal distribution of model-specific annual mean wetland CH_4 emission estimates during the 2008–2017 period (a). Solid lines and shaded areas represent the mean and range of wetland CH_4 emission estimates from individual model groups, respectively. The distribution of annual mean wetland CH_4 emission estimates among all model-years from 2008 to 2017 (b). The open circle, bottom edge, and top edge of the black box in each violin plot indicate the 50th, 25th, and 75th percentiles of the inferred global wetland CH_4 emission estimates, respectively. The wetland CH_4 emission maps inferred from the BU and TD models (c), the BU models (d), the TD models (e), and the machine learning model ($UPCH_4$; f) during the 2008–2017 period. The FLUXNET-CH_4 freshwater wetland sites used in this study are denoted as blue open circles in (f).

(e.g., biosphere-atmosphere fluxes), land cover properties (e.g., vegetation type and phenology), and soil properties (e.g., soil type) synthesized from FLUXNET-CH_4 in situ measurements and remote sensing products (McNicol et al., Submitted). Like the BU- and TD-based global emission estimates, the wetland CH_4 emission density per gridcell area reported in the $UPCH_4$ dataset was converted to wetland CH_4 emission density per wetland area with the WAD2M wetland area and dynamics dataset (Zhang et al., 2021). We compared the wetland CH_4 emission patterns prescribed by the $UPCH_4$ dataset against other existing datasets, and assessed the potential of using $UPCH_4$ data to refine BU- and TD-based wetland CH_4 emission estimates.

2.5 | The ILAMB system

We employed the ILAMB framework to evaluate the present state of global wetland CH_4 modeling based on site-level FLUXNET-CH_4 observations and global gridded simulation products. ILAMB is an open-source model benchmarking software package that performs comprehensive model assessment (e.g., period mean, bias, seasonal cycle) across a wide range of observations and generates graphical diagnostics (e.g., spatial contour maps and Taylor diagrams; Collier et al., 2018). The ILAMB software package has been adopted by model development and intercomparison projects to keep track of land model performance among models and model versions (Lawrence et al., 2019).

We use ILAMB for benchmarking models at both the site and global scales. ILAMB produces overall scores consisting of normalized values synthesizing model performance across a range of dimensions with respect to a given dataset, ranging from zero (worst) to one (best). The site-level ILAMB overall scores presented in this study consist of model evaluations of bias, root-mean-square error (RMSE), and seasonal cycles conducted at individual wetland sites, and the global-scale ILAMB overall scores also evaluates the modeled spatial distributions (Collier et al., 2018). The ILAMB overall scores inferred from individual reference datasets were paired with model-specific global wetland CH_4 emission estimates to assess the potential of reducing prediction spreads with better-performing models. Importantly, the model performance scores reported in this study are subjective to the selected reference datasets and should thus not be interpreted as a model ranking (Seiler et al., 2021).

2.6 | Experimental design

We implemented the ILAMB framework (Collier et al., 2018) to evaluate site-level and global-scale wetland CH_4 emission estimates inferred from 14 BU biogeochemical models (Table S2), nine TD models (22 inversions, Table S3), and one ML model. Gridded outputs collected from different model products were remapped onto the same 1 degree by 1 degree (for model evaluation) and 0.25 degree by 0.25 degree (for global wetland CH_4 emission calculation) global gridcells using the NetCDF Operators (NCO; Zender, 2008).

The site-scale assessment was performed by evaluating wetland CH_4 emissions inferred from BU, TD, and ML models at gridcells containing FLUXNET-CH_4 wetland sites whenever the measurements were available. We grouped the FLUXNET-CH_4 sites by their location and ecosystem type to assess the sensitivity of model performance score to the selection of benchmarking dataset. The resulting eight sets of observational constraints are (1) measurements collected from all sites across the globe (42 sites), (2) measurements collected from north of 30°N (34 sites), (3) measurements collected from south of 30°N (8 sites), (4) measurements collected from bog sites across the globe (8 sites), (5) measurements collected from fen sites across the globe (8 sites), (6) measurements collected from marsh sites across the globe (10 sites), (7) measurements collected from swamp sites across the globe (6 sites), and (8) measurements collected from wet tundra sites across the globe (11 sites).

The global-scale assessment was performed by evaluating BU- and TD-based model outputs against the global gridded $UPCH_4$ dataset during the 2008 to 2017 period when wetland CH_4 emission estimates are available for most of the BU and TD models analyzed in this study. As described in Section 2.4, the $UPCH_4$ dataset employed machine learning methods to extrapolate ecosystem-scale wetland CH_4 emission observations into global-scale emission predictions, which is currently the only gridded wetland CH_4 emission estimates inferred from observed functional relationships. We note here that the robustness of the global-scale assessment is subject to the reliability of the $UPCH_4$ dataset, which should be interpreted as a sensitivity test to measurement extrapolation.

Model performance was estimated by calculating model-specific ILAMB overall scores for each wetland CH_4 emission reference dataset. The relationship between model performance and global wetland CH_4 emission estimates was examined by analyzing the prediction ranges inferred from the top 50%, 40%, 30%, and 20% BU and TD models determined by the cumulative distribution function of their ILAMB overall scores.

We note that the BU and TD global wetland CH_4 emission estimates calculated in this study are not identical to those reported in Saunois et al. (2020) due to differences in model collection and data processing (e.g., remapping scheme, land area map, and spatial resolution). We also note a unit conversion error (model outputs reported in TgC year^{-1} but read in as $TgCH_4$ year^{-1}) for the TRIPLEX-GHG model, whose global wetland CH_4 emission estimates should be 136 $TgCH_4$ year^{-1} instead of the 102 $TgCH_4$ year^{-1} reported in Saunois et al. (2020).

3 | RESULTS AND DISCUSSION

3.1 | Present state of global wetland CH_4 modeling

Comparison at the global scale show the latitudinal distributions of wetland CH_4 emissions inferred from BU and TD models both suggest that tropical wetlands dominate global wetland CH_4 emission estimates (Figure 1a). This dominant tropical emission pattern does not exist in the ML model estimates, a discrepancy likely driven by the low wetland CH_4 emissions recorded in the few existing tropical wetland eddy covariance measurements (Figure 2a). There are 140, 187, and 10 model-years during the 2008 to 2017 period in BU, TD, and ML models, respectively, and the modeled mean annual global wetland CH_4 emission estimates are highest in the TD models and lowest in the ML model (Figure 1b). The wide range of predictions inferred from BU models covers most of the TD- and ML-based estimates, demonstrating the need to evaluate the relationship between model performance and modeled global wetland CH_4 emission estimates. The multi-model ensemble means inferred from BU and TD models (Figures 1c–e) have similar global distribution patterns, with higher emissions in South America and lower emissions in the Sahel and Australia than those from the ML model (Figure 1f).

Our site-level evaluation conducted at the 42 FLUXNET-CH_4 sites shows that wetland CH_4 emissions estimated by TD models are on average larger (with relatively wider prediction ranges) than those inferred from observations except for regions within 36° to 40°N (Figure 2a). The median wetland CH_4 emission estimates inferred from BU models are comparable to observations, although the prediction ranges vary substantially across latitudes. Wetland CH_4 emission estimates extracted from the $UPCH_4$ dataset align closely with observations, since the same set of measurements were used to train the ML model. While site-level measurements may not represent all wetland types and conditions in the corresponding model gridcell, these observations provide valuable benchmarks for BU and TD model developments. In particular, the wide ranges of wetland CH_4 emission estimates inferred from individual model gridcells highlight the need to refine the large inter-model variability not driven by wetland area estimates or climate forcing uncertainties. Overall, at these sites, observed wetland CH_4 emission density ($mgCH_4$ m^{-2} day^{-1}) is overestimated by all the examined model groups (Figure 2b). The TD models estimate the highest mean wetland CH_4 emission density over the 42 sites (107 $mgCH_4$ m^{-2} day^{-1}), followed by the BU (63 $mgCH_4$ m^{-2} day^{-1}) and ML models (46 $mgCH_4$ m^{-2} day^{-1}). We note that the comparisons presented here are heavily biased toward high-latitude measurements where FLUXNET-CH_4 sites are relatively denser, and therefore may not accurately represent global wetland

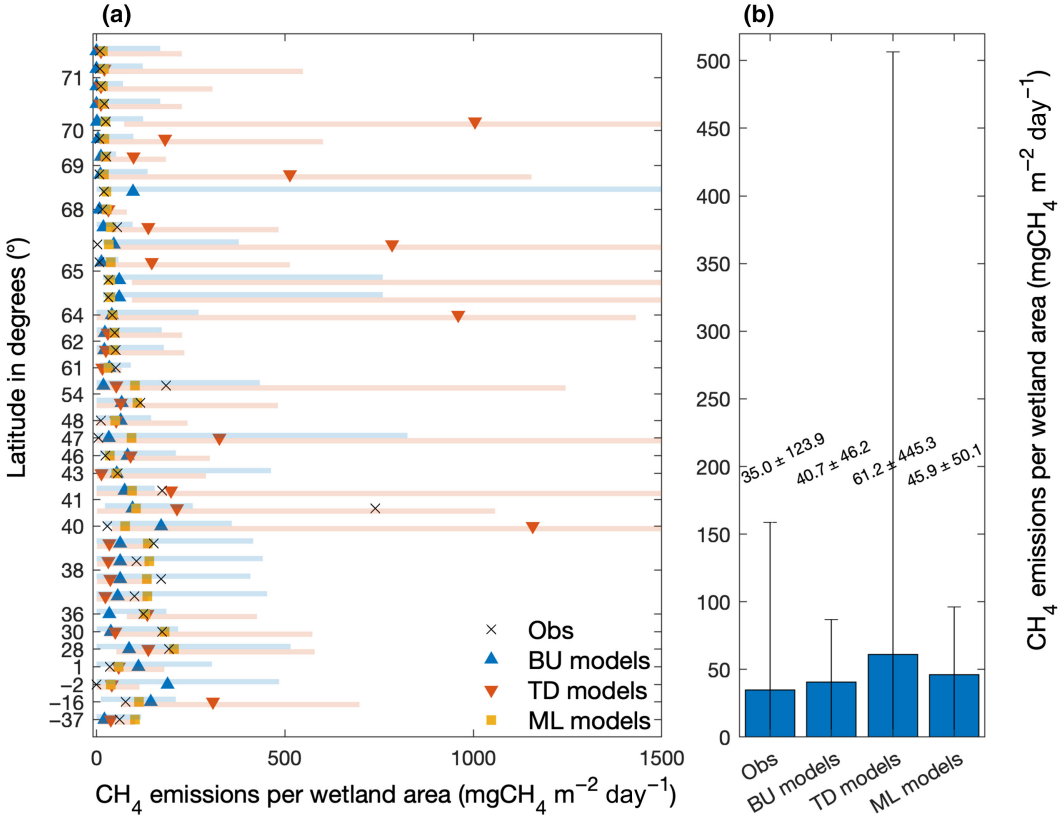

FIGURE 2 Site-level comparison of observed and simulated wetland CH_4 emission density. The site-specific mean wetland CH_4 emissions per m^2 of wetland inferred from observations (black crosses), BU biogeochemical models (blue triangles), TD atmospheric inversion models (red triangles), and the UPCH$_4$ dataset (yellow squares) over the years when daily gap-filled wetland CH_4 emission density (FCH$_4$_F_ANN_mean) were available in the FLUXNET-CH_4 database (a). Symbols and shaded areas represent the median and range across the BU (blue) and TD (red) models, respectively. The TD model results were not shown at US-Ivo (68.49°N) due to unrealistically large emission estimates (Figure S4). Sites are sorted by latitudes and only latitudes where sites are located are labeled. The mean and standard deviation across the 42 FLUXNET-CH_4 freshwater wetland sites, calculated from site measurements, BU model ensemble, and TD model ensemble (b).

CH_4 emission patterns. Furthermore, models may not accurately represent site-level mean wetland CH_4 emissions over the 2008 to 2017 period (Figure S3).

3.2 | Accuracy of wetland CH_4 modeling

We quantified the performance of the BU, TD, and ML models by evaluating their bias, RMSE, and seasonal cycles against global FLUXNET-CH_4 measurements through ILAMB (Figure 3). The ILAMB overall scores integrate the bias, RMSE, and seasonal cycles benchmarking results into a single metric that quantitatively synthesizes model performance (Figure S5). Our results show that (1) models with finer grids do not necessarily show an improved model performance (comparable performance inferred from 0.25° and 1° outputs from the ML model); (2) the performance of BU models may not be determined by the complexity of the biogeochemical process representations; and (3) the performance of TD models is sensitive to the associated atmospheric CH_4 observation (e.g., CarbonTracker Europe-CH_4 performs better with the GOSAT product; Figure 3a). Overall, ML models have the highest ILAMB overall scores against FLUXNET-CH_4 measurements, likely because the same set of measurements were used during ML model development.

While the ILAMB overall score synthesizes the comparison of multiple model performance measures, the underlying calculation of model performance scores may smooth out the differences between observations and simulations. For example, the variability of ILAMB overall scores (Figure 3a) is much weaker than the variability of the modeled wetland CH_4 emission density across all sites (Figure 2a). Developing a normalization scheme that provides discernible model performance labels could improve the interpretation of model scores provided by model-data intercomparison packages like ILAMB. While the current ILAMB scoring normalization contributes to the low standard deviation of ILAMB overall scores within the same model group, the distribution of ILAMB overall scores suggests that BU models generally perform better than TD models at these 42 freshwater wetland sites (Figure 3b).

The BU and TD models were categorized into the top 50%, top 40%, top 30%, and top 20% model performance groups by the cumulative distribution function of their ILAMB overall scores, effectively capturing models that better represent site-level measurements (Figure S6). For both BU and TD models, the range of

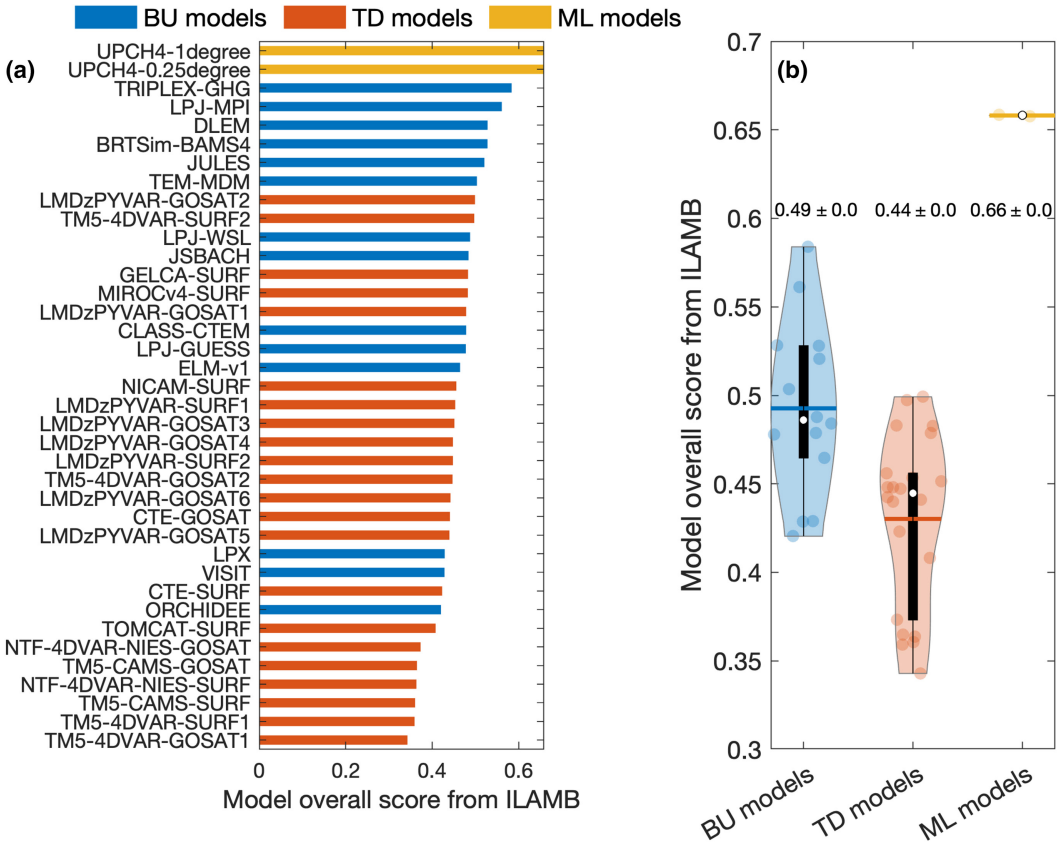

FIGURE 3 Present state of global wetland CH_4 modeling evaluated by FLUXNET-CH_4 measurements at 42 sites. The ILAMB overall scores for bottom-up (BU) biogeochemical models, top-down (TD) atmospheric inversion models, and a machine learning (ML) upscaling model over the years when FLUXNET-CH_4 measurements were available (a). The distribution of ILAMB overall scores inferred for individual model groups (b). The open circle, bottom edge, and top edge of the black box in each violin plot indicate the 50th, 25th, and 75th percentiles of the inferred ILAMB overall scores, respectively. The number above each violin plot represents the mean ± standard deviation of the corresponding ILAMB overall score distribution.

modeled global wetland CH_4 emission estimates becomes narrower with the use of the top 50% (or better) models (Figure 4a). Using the top 20% models reduces the prediction spread of wetland CH_4 emission estimates by 62% and 39% for BU- and TD-based approaches, respectively. Nevertheless, the ensemble means of global wetland CH_4 emission estimates based on model meritocracy (i.e., the top 20%–50% models) were comparable to those from model democracy (i.e., all models), as their differences (the top 20%–50% models vs. all models) were <3% for both BU and TD models. The discrepancies between BU- and TD-based multi-model mean global wetland CH_4 emission estimates increased by 5 $TgCH_4$ $year^{-1}$ when the top 20% models were used. When model performance was evaluated using the $UPCH_4$ dataset, both the prediction spread within BU and TD models and the discrepancies between BU- and TD-based multi-model mean global wetland CH_4 emission estimates were reduced (Figure 4b). These results demonstrate that while applying model meritocracy has the potential to reduce the spread of wetland CH_4 emission estimates within individual model groups, the refined estimates are sensitive to the selection of reference dataset. Future research should attempt to integrate new benchmarks that can elucidate TD priors and inversion approaches or BU model functional responses, for example, CH_4 emission sensitivity to temperature (Chang et al., 2021) and water table depth (Goodrich et al., 2015), to further evaluate the potential of applying a model meritocracy to global wetland CH_4 emission estimation.

3.3 | Sensitivity to reference datasets

For each model, the large ILAMB overall score sensitivity to reference dataset selection suggests that model development aiming to improve model performance against a given benchmark is subject to the availability of existing constraints (Figure 5). Our analyses indicate that model benchmarking results depend on the geographic location and ecosystem type represented in the observational constraints. For example, different sets of best-performing models were identified when benchmarking against sites north or south of 30°N, except for the ML models derived from both sets of measurements. We also note that the ILAMB overall scores inferred from BU models are generally higher than those from TD models at the bog, fen, and wet tundra sites, and generally lower at the swamp sites. Such benchmarking sensitivities to site representation highlight the

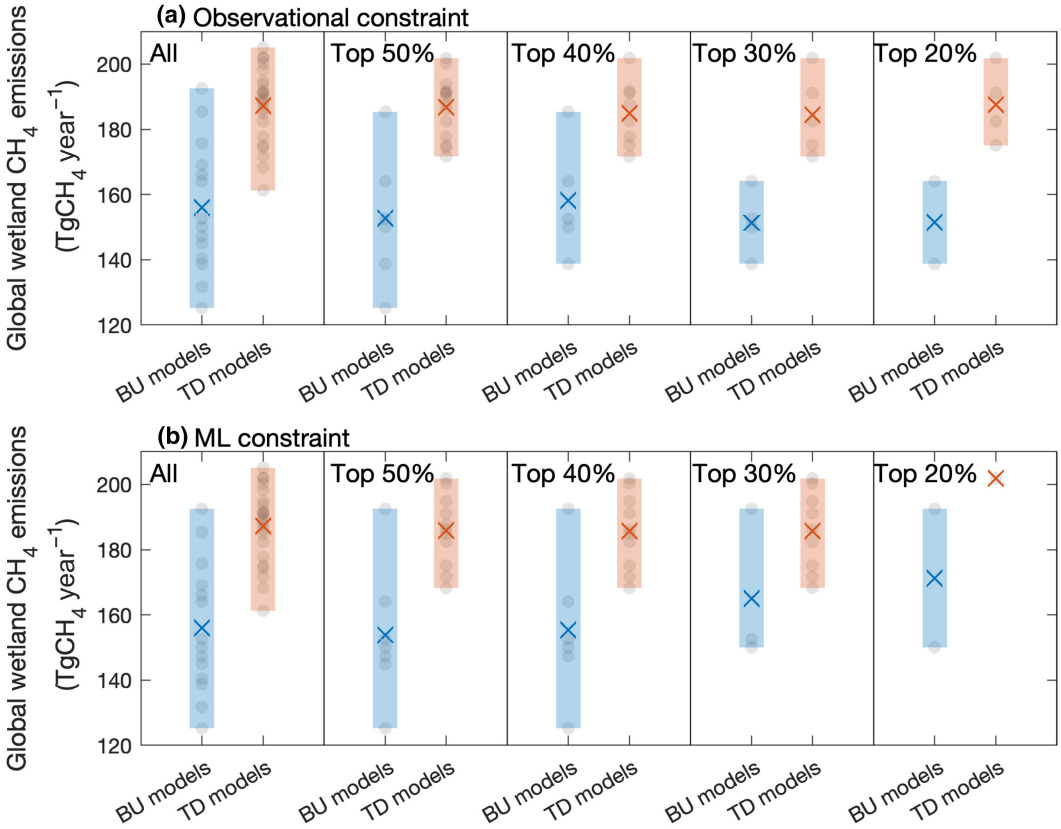

FIGURE 4 The comparison of global wetland CH_4 emission estimates inferred from models with different accuracy groups evaluated by site-level FLUXNET-CH_4 measurements (a) and the global gridded $UPCH_4$ dataset that upscales FLUXNET-CH_4 measurements with machine learning techniques (b). The dots, crosses, and shaded area represent the ensemble members, mean, and range of the BU (blue) and TD (red) models for each accuracy group, respectively. [Colour figure can be viewed at wileyonlinelibrary.com]

importance of systematically observing and evaluating wetland biogeochemistry across latitudes and ecosystems, especially for wetlands south of 30°N that account about 75% of global wetland CH_4 emissions (Saunois et al., 2020).

When evaluated against the global gridded $UPCH_4$ dataset, the BU models generally have higher ILAMB overall scores than the TD models. Importantly, the higher ILAMB overall scores inferred from the BU models may not necessarily indicate better representation of global wetland CH_4 emissions, since independent gridded observations are still lacking to evaluate model performance at the global scale. Although the representativeness of data-driven models is limited by available observational constraints, estimates derived from novel model-data integration schemes still provide valuable insights on global wetland CH_4 emission estimates due to the lack of a globally gridded measurement network. Recognizing limitations embedded in individual reference datasets is needed to refine wetland CH_4 emission estimates with performance-based model weighting (Brunner et al., 2020; Knutti et al., 2017). Additionally, applying multiple validated constraints for model evaluation could improve the robustness of the inferred model performance, as no single BU or TD model can outperform other models across all the examined reference datasets. Our results thus encourage future model development to employ benchmarking tools like ILAMB to systematically evaluate model performance against multiple reference datasets to ensure model improvement during each update.

While the FLUXNET-CH_4 dataset provides valuable observational constraints at site-level scales, the current distribution of sites makes it challenging to serve as a benchmark for global wetland CH_4 emission estimates. For example, the weak correlation between site-level wetland CH_4 emission measurements and global-scale wetland CH_4 emission estimates indicates that the current FLUXNET-CH_4 dataset may not adequately characterize global wetland CH_4 emission estimates (Figure S7). One potential reason inhibiting the use of site-level observations to constrain global-scale estimates is the incomplete representation of wetland characteristics (e.g., insufficient measurements of wetlands under diverse environmental conditions), which is unlikely to improve in the near future unless direct interventions are taken to fill the gaps in the network. The representativeness analysis conducted in Delwiche et al. (2021) suggests that the freshwater wetland sites in the current FLUXNET-CH_4 dataset only sparsely cover humid tropical regions, demonstrating the need to improve data coverage in tropical and subtropical wetlands. Besides assessing goodness of fit against available wetland CH_4 observations, future model benchmarking studies should consider analyzing observed functional relationships that may be transferable across sites. For example, evaluating how modeled wetland

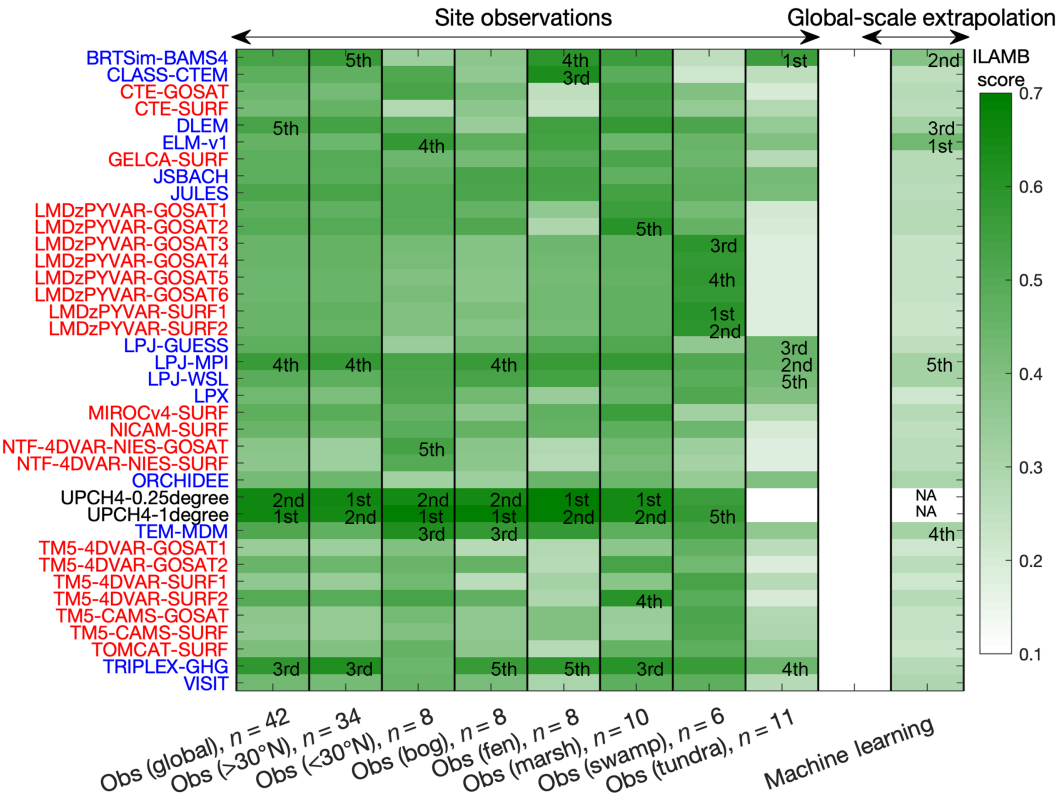

FIGURE 5 Model-specific ILAMB overall scores against the selection of the reference dataset. Columns represent the ILAMB overall scores inferred from different sets of reference data, including measurements taken at eight groups of FLUXNET-CH_4 sites: across the globe (Obs, global), north of 30°N (Obs, >30°N), south of 30°N (Obs, <30°N), bog sites (Obs, bog), fen sites (Obs, fen), marsh sites (Obs, marsh), swamp sites (Obs, swamp), and wet tundra sites (Obs, tundra) and the $UPCH_4$ dataset (machine learning). BU and TD models are labeled by blue and red on the *y*-axis, respectively. [Colour figure can be viewed at wileyonlinelibrary.com]

CH_4 emission estimates respond to variations in water table dynamics (Goodrich et al., 2015), substrate and microbial dynamics (Chang et al., 2021; Mitra et al., 2020), and carbon uptake dynamics (Rinne et al., 2018) could provide further constraints without introducing additional wetland CH_4 observations. In parallel, the development of causality-guided (Yuan et al., 2022) and knowledge-guided (Willard et al., 2020) ML products also have the potential to improve the description of global-scale wetland CH_4 emission patterns and thereby reconcile the prediction spread across models.

3.4 | A framework toward refining global wetland CH_4 emissions

Applying observational constraints generally reduces the range of global wetland CH_4 emission estimates for both BU and TD models (i.e., narrower prediction spreads within the same model group), except for BU estimates inferred from measurements south of 30°N and TD estimates inferred from wet tundra measurements (Figure 6a). Our results suggest that the reduced BU and TD prediction spreads may not be directly attributed to improved model performance, because the ILAMB overall score and global wetland CH_4 emission estimates are largely decoupled for both BU- and TD-based approaches (Figure S8). Such a weak correlation indicates that none of the best-available constraints can sufficiently reconcile the differences between the ensemble mean of global wetland CH_4 emission estimates inferred from the best-performing BU and TD models, emphasizing the need to further develop reference datasets capable of adequately linking model performance with global emissions.

Nevertheless, global wetland CH_4 emission estimates are sensitive to the definition of better-performing models (Figure 4) and the selection of benchmarking dataset (Figure 6a). We therefore explored the most likely global wetland CH_4 emission estimates based on the probability density function of estimates inferred from the top 20% BU and TD models identified by the eight constraints examined in this study (Figure 6b). The most likely global wetland CH_4 emission estimates are about 143 $TgCH_4$ $year^{-1}$ and 188 $TgCH_4$ $year^{-1}$ for BU- and TD-based estimates, respectively (Figure 6b). Our results show that bootstrapping the top 20% BU and TD model estimates with 1000 resampling narrows the distribution of global wetland CH_4 emission estimates (Figure 6c), demonstrating the potential of reducing BU- and TD-based prediction spreads with further observational constraints. While such a probability-based framework should be less sensitive to uncertainties embedded in any particular ensemble member and underlying constraint, the robustness of the benchmarking approach relies on the representativeness of the measurement samples and the inferred observational constraints.

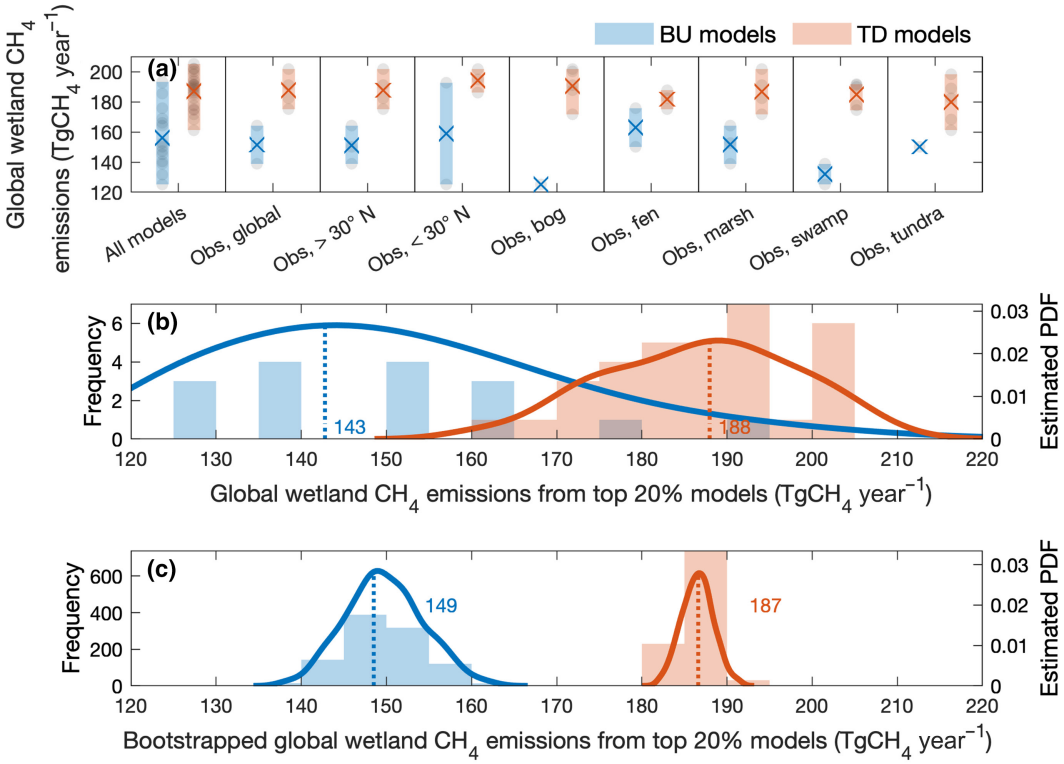

FIGURE 6 The distribution of global wetland CH_4 emission estimates from all available bottom-up (BU) and top-down (TD) models (all models) and the top 20% BU and TD models inferred from eight groups of FLUXNET-CH_4 measurements (Obs; a). The dots, crosses, and shaded area represent the ensemble members, mean, and range of the BU (blue) and TD (red) models for each group, respectively. The probability density function (lines) and frequency distribution (bars) of global wetland CH_4 emission estimates from the top 20% BU and TD models (b) and the corresponding bootstrapped dataset from 1000 resampling (c). [Colour figure can be viewed at wileyonlinelibrary.com]

To improve data availability, the framework is built on open-source ILAMB software that allows modeling groups to systematically refine global wetland CH_4 emission estimates with future advances in CH_4 observations and simulations.

4 | CONCLUSIONS

The wide range of global wetland CH_4 emission estimates from different model approaches indicates the need to reduce uncertainties in current wetland CH_4 modeling by integrating reference datasets using tools like the open-source software ILAMB system. Our analyses demonstrate the potential of selecting better-performing models relative to reference data to refine global wetland CH_4 emission estimates. This approach reduced the prediction spread of BU and TD global wetland CH_4 emission estimates by 62% and 39%, respectively. However, global BU and TD CH_4 emission estimate discrepancies slightly increased (from 31 to 36 $TgCH_4$ $year^{-1}$) when the top 20% models were used, although we consider such discrepancies sensitive to the wetland characteristics captured in current observations. Importantly, the interpretation of model performance is sensitive to the choice of observational constraints, suggesting that static benchmarking with current observations alone may not be sufficient enough to guide wetland CH_4 model development. Careful evaluation of benchmarking metrics and tools is needed to move beyond the limitations of model democracy (Hausfather et al., 2022). The evaluation framework demonstrated in this study can readily accept expanded CH_4 observations and improved simulations to systematically refine our estimates of global wetland CH_4 emission budgets.

ACKNOWLEDGMENTS

This study was funded by the RUBISCO SFA of the Regional and Global Modeling Analysis (RGMA)and the E3SM program in the U.S. Department of Energy Office of Science under contract DE-AC02-05CH11231. This work was also conducted as a part of the Wetland FLUXNET Synthesis for Methane Working Group supported by the John Wesley Powell Center for Analysis and Synthesis of the U.S. Geological Survey. The compilation of the FLUXNET-CH_4 data is supported by the Gordon and Betty Moore Foundation through Grant GBMF5439 "Advancing Understanding of the Global Methane Cycle" to Stanford University supporting the Methane Budget activity for the Global Carbon Project (globalcarbonproject.org). We acknowledge the FLUXNET-CH_4 community product (Delwiche et al., 2021) and Global Carbon Project CH_4 modeling group (Saunois et al., 2020) for the data provided in this analysis. We thank Peter Bergamaschi for sharing the TM5-CAMS model data used in this study. FJ acknowledges support by the Swiss National

Science Foundation (#200020_200511). FM and CP acknowledge the National Computational Infrastructure of the National Computational Infrastructure of the Australian Government through the NCMAS Allocation Scheme (grant NCMAS-2021-78), and the Sydney Informatics Hub HPC Allocation Scheme supported by the Office of the Deputy Vice-Chancellor (Research). N.G. acknowledges support from the Newton Fund through the Met Office Climate Science for Service Partnership Brazil (CSSP Brazil).

DATA AVAILABILITY STATEMENT

The FLUXNET-CH_4 community product can be downloaded from https://fluxnet.org/data/fluxnet-ch4-community-product/. The modeling data contributed to the 2008–2017 global CH_4 budget are available from ICOS (doi: 10.18160/gcp-ch4-2019). The benchmarking and modeling data analyzed in this study can be downloaded at https://zenodo.org/record/7880014.

CODE AVAILABILITY

The source code, including usage tutorials, of the ILAMB system can be downloaded from https://github.com/rubisco-sfa/ILAMB.

ORCID

Kuang-Yu Chang https://orcid.org/0000-0002-7859-5871
Benjamin Poulter https://orcid.org/0000-0002-9493-8600

REFERENCES

Allen, M. R., Shine, K. P., Fuglestvedt, J. S., Millar, R. J., Cain, M., Frame, D. J., & Macey, A. H. (2018). A solution to the misrepresentations of CO_2-equivalent emissions of short-lived climate pollutants under ambitious mitigation. *NPJ Climate and Atmospheric Science*, *1*(1), 1–8.

Balcombe, P., Speirs, J. F., Brandon, N. P., & Hawkes, A. D. (2018). Methane emissions: Choosing the right climate metric and time horizon. *Environmental Science. Processes & Impacts*, *20*(10), 1323–1339.

Bohn, T. J., Melton, J. R., Ito, A., Kleinen, T., Spahni, R., Stocker, B. D., Zhang, B., Zhu, X., Schroeder, R., Glagolev, M. V., Maksyutov, S., Brovkin, V., Chen, G., Denisov, S. N., Eliseev, A. V., Gallego-Sala, A., McDonald, K. C., Rawlins, M. A., Riley, W. J., … Kaplan, J. O. (2015). WETCHIMP-WSL: Intercomparison of wetland methane emissions models over West Siberia. *Biogeosciences*, *12*(11), 3321–3349.

Brunner, L., Pendergrass, A. G., Lehner, F., Merrifield, A. L., Lorenz, R., & Knutti, R. (2020). Reduced global warming from CMIP6 projections when weighting models by performance and Independence. *Earth System Dynamics*, *11*, 995–1012.

Chadburn, S. E., Aalto, T., Aurela, M., Baldocchi, D., Biasi, C., Boike, J., Burke, E. J., Comyn-Platt, E., Dolman, A. J., Duran-Rojas, C., Fan, Y., Friborg, T., Gao, Y., Gedney, N., Göckede, M., Hayman, G. D., Holl, D., Hugelius, G., Kutzbach, L., … Westermann, S. (2020). Modeled microbial dynamics explain the apparent temperature sensitivity of wetland methane emissions. *Global Biogeochemical Cycles*, *34*(11). https://doi.org/10.1029/2020GB006678

Chang, K.-Y., Riley, W. J., Brodie, E. L., McCalley, C. K., Crill, P. M., & Grant, R. F. (2019). Methane production pathway regulated proximally by substrate availability and distally by temperature in a high-latitude mire complex. *Journal of Geophysical Research: Biogeosciences*, *124*(10), 3057–3074.

Chang, K.-Y., Riley, W. J., Crill, P. M., Grant, R. F., & Saleska, S. R. (2020). Hysteretic temperature sensitivity of wetland CH_4 fluxes explained by substrate availability and microbial activity. *Biogeosciences*, *17*(22), 5849–5860.

Chang, K.-Y., Riley, W. J., Knox, S. H., Jackson, R. B., McNicol, G., Poulter, B., Aurela, M., Baldocchi, D., Bansal, S., Bohrer, G., Campbell, D. I., Cescatti, A., Chu, H., Delwiche, K. B., Desai, A. R., Euskirchen, E., Friborg, T., Goeckede, M., Helbig, M., … Zona, D. (2021). Substantial hysteresis in emergent temperature sensitivity of global wetland CH(4) emissions. *Nature Communications*, *12*(1). https://doi.org/10.1038/s41467-021-22452-1

Chu, H., Luo, X., Zutao Ouyang, W., Chan, S., Dengel, S., Biraud, S. C., Torn, M. S., Metzger, S., Kumar, J., Arain, M. A., & Arkebauer, T. J. (2021). Representativeness of Eddy-covariance flux footprints for areas surrounding AmeriFlux sites. *Agricultural and Forest Meteorology*, *301*, 108350. https://doi.org/10.1016/j.agrformet.2021.108350

Collier, N., Hoffman, F. M., Lawrence, D. M., Keppel-Aleks, G., Koven, C. D., Riley, W. J., Mingquan, M., & Randerson, J. T. (2018). The international land model benchmarking (ILAMB) system: Design, theory, and implementation. *Journal of Advances in Modeling Earth Systems*, *10*(11), 2731–2754.

Delwiche, K. B., Knox, S. H., Malhotra, A., Fluet-Chouinard, E., McNicol, G., Feron, S., Ouyang, Z., Papale, D., Trotta, C., Canfora, E., Cheah, Y.-W., Christianson, D., Alberto, M. C. R., Alekseychik, P., Aurela, M., Baldocchi, D., Bansal, S., Billesbach, D. P., Bohrer, G., … Jackson, R. B. (2021). FLUXNET-CH_4: A global, multi-ecosystem dataset and analysis of methane seasonality from freshwater wetlands. *Earth System Science Data*, *13*(7), 3607–3689.

Goodrich, J. P., Campbell, D. I., Roulet, N. T., Clearwater, M. J., & Schipper, L. A. (2015). Overriding control of methane flux temporal variability by water table dynamics in a southern hemisphere, raised bog. *Journal of Geophysical Research: Biogeosciences*, *120*(5), 819–831.

Grant, R. F., Mekonnen, Z. A., Riley, W. J., Arora, B., & Torn, M. S. (2019). Modeling climate change impacts on an Arctic polygonal tundra: 2. Changes in CO_2 and CH_4 exchange depend on rates of permafrost thaw as affected by changes in vegetation and drainage. *Journal of Geophysical Research: Biogeosciences*, *124*, 1323–1341. https://doi.org/10.1029/2018jg004645

Harris, I. C. (2019). CRU JRA v1. 1: A Forcings dataset of gridded land surface blend of climatic research unit (CRU) and Japanese reanalysis (JRA) data, January 1901–December 2017, University of East Anglia Climatic Research Unit, Centre for Environmental Data Analysis. *Centre for Environmental Data Analysis P* 2905.

Hausfather, Z., Marvel, K., Schmidt, G. A., Nielsen-Gammon, J. W., & Zelinka, M. (2022). Climate simulations: Recognize the 'hot model' problem. *Nature*, *605*, 2022–2029. https://doi.org/10.1038/d41586-022-01192-2

Hemes, K. S., Chamberlain, S. D., Eichelmann, E., Knox, S. H., & Baldocchi, D. D. (2018). A biogeochemical compromise: The high methane cost of sequestering carbon in restored wetlands. *Geophysical Research Letters*, *45*(12), 6081–6091.

Houweling, S., Bergamaschi, P., Chevallier, F., Heimann, M., Kaminski, T., Krol, M., Michalak, A. M., & Patra, P. (2017). Global inverse modeling of CH_4 sources and sinks: An overview of methods. *Atmospheric Chemistry and Physics*, *17*(1), 235–256.

Inoue, M., Morino, I., Uchino, O., Nakatsuru, T., Yoshida, Y., Yokota, T., Wunch, D., Wennberg, P. O., Roehl, C. M., Griffith, D. W. T., Velazco, V. A., Deutscher, N. M., Warneke, T., Notholt, J., Robinson, J., Sherlock, V., Hase, F., Blumenstock, T., Rettinger, M., … Tanaka, T. (2016). Bias corrections of GOSAT SWIR XCO_2 and XCH_4 with TCCON data and their evaluation using aircraft measurement data. *Atmospheric Measurement Techniques*, *9*(8), 3491–3512.

IPCC. (2021). Climate change 2021: The physical science basis. In: V. Masson-Delmotte, P. Zhai, A. Pirani, S. L. Connors, C. Péan, S. Berger, N. Caud, Y. Chen, L. Goldfarb, M. I. Gomis, M. Huang, K. Leitzell, E. Lonnoy, J. B. R. Matthews, T. K. Maycock, T. Waterfield, O. Yelekçi, R. Yu, & B. Zhou (Eds.), *Contribution of working group I to the sixth assessment report of the intergovernmental panel on climate change*. Cambridge: Cambridge University Press. https://doi.org.10.1017/9781009157896

Jackson, R. B., Saunois, M., Bousquet, P., Canadell, J. G., Poulter, B., Stavert, A. R., Bergamaschi, P., Niwa, Y., Segers, A., & Tsuruta, A. (2020). Increasing anthropogenic methane emissions arise equally from agricultural and fossil fuel sources. *Environmental Research Letters*, *15*(7), 071002.

Kirschke, S., Bousquet, P., Ciais, P., Saunois, M., Canadell, J. G., Dlugokencky, E. J., Bergamaschi, P., Bergmann, D., Blake, D. R., Bruhwiler, L., Cameron-Smith, P., Castaldi, S., Chevallier, F., Feng, L., Fraser, A., Heimann, M., Hodson, E. L., Houweling, S., Josse, B., … Zeng, G. (2013). Three decades of global methane sources and sinks. *Nature Geoscience*, *6*(10), 813–823.

Knox, S. H., Bansal, S., McNicol, G., Schafer, K., Sturtevant, C., Ueyama, M., Valach, A. C., Baldocchi, D., Delwiche, K., Desai, A. R., Euskirchen, E., Liu, J., Lohila, A., Malhotra, A., Melling, L., Riley, W., Runkle, B. R. K., Turner, J., Vargas, R., … Jackson, R. B. (2021). Identifying dominant environmental predictors of freshwater wetland methane fluxes across diurnal to seasonal time scales. *Global Change Biology*, *27*(15), 3582–3604.

Knox, S. H., Jackson, R. B., Poulter, B., McNicol, G., Fluet-Chouinard, E., Zhang, Z., Hugelius, G., Bousquet, P., Canadell, J. G., Saunois, M., & Papale, D. (2019). FluXNET-CH_4 synthesis activity objectives, observations, and future directions. *Bulletin of the American Meteorological Society*, *100*(12), 2607–2632.

Knutti, R., Sedláček, J., Sanderson, B. M., Lorenz, R., Fischer, E. M., & Eyring, V. (2017). A climate model projection weighting scheme accounting for performance and interdependence. *Geophysical Research Letters*. https://doi.org/10.1002/2016gl072012

Lan, X., Thoning, K. W., & Dlugokencky, E. J. Trends in globally-averaged CH4, N2O, and SF6 determined from NOAA Global Monitoring Laboratory measurements. Version 2023–04. https://doi.org/10.15138/P8XG-AA10

Lawrence, D. M., Fisher, R. A., Koven, C. D., Oleson, K. W., Swenson, S. C., Bonan, G., Collier, N., Ghimire, B., van Kampenhout, L., Kennedy, D., Kluzek, E., Lawrence, P. J., Li, F., Li, H., Lombardozzi, D., Riley, W. J., Sacks, W. J., Shi, M., Vertenstein, M., … Zeng, X. (2019). The community land model version 5: Description of new features, benchmarking, and impact of forcing uncertainty. *Journal of Advances in Modeling Earth Systems*, *11*(12), 4245–4287.

Ma, S., Worden, J. R., Anthony Bloom, A., Zhang, Y., Poulter, B., Cusworth, D. H., Yin, Y., Pandey, S., Maasakkers, J. D., Lu, X., & Shen, L. (2021). Satellite constraints on the latitudinal distribution and temperature sensitivity of wetland methane emissions. *AGU Advances*, *2*(3), e2021AV000408.

Maasakkers, J. D., Jacob, D. J., Sulprizio, M. P., Scarpelli, T. R., Nesser, H., Sheng, J., Zhang, Y., Lu, X., Bloom, A. A., Bowman, K. W., Worden, J. R., & Parker, R. J. (2021). 2010–2015 north American methane emissions, sectoral contributions, and trends: A high-resolution inversion of GOSAT observations of atmospheric methane. *Atmospheric Chemistry and Physics*, *21*, 4339–4356. https://doi.org/10.5194/acp-21-4339-2021

McNicol, G., Fluet-Chouinard, E., Ouyang, Z., Knox, S., Zhang, Z., Poulter, B., Jackson, R. B., Aalto, T., Bansal, S., Delwiche, K., Feron, S., Goeckede, M., Liu, J., Chang, K.-Y., Malhotra, A., Melton, J. R., Riley, W., Vargas, R., & Zhu, Q. UpCH_4: A global freshwater wetland methane emissions product for 2001–2018 from upscaled eddy covariance fluxes, Submitted. *AGU Advances*.

Melton, J. R., Wania, R., Hodson, E. L., Poulter, B., Ringeval, B., Spahni, R., Bohn, T., Avis, C. A., Beerling, D. J., Chen, G., Eliseev, A. V., Denisov, S. N., Hopcroft, P. O., Lettenmaier, D. P., Riley, W. J., Singarayer, J. S., Subin, Z. M., Tian, H., Zürcher, S., … Kaplan, J. O. (2013). Present state of global wetland extent and wetland methane modelling: Conclusions from a model inter-comparison project (WETCHIMP). *Biogeosciences*, *10*(2), 753–788.

Mitra, B., Minick, K., Miao, G., Domec, J. C., Prajapati, P., McNulty, S. G., Sun, G., King, J. S., & Noormets, A. (2020). Spectral evidence for substrate availability rather than environmental control of methane emissions from a coastal forested wetland. *Agricultural and Forest Meteorology*, *291*(2019), 108062.

Morin, T. H., Bohrer, G., Stefanik, K. C., Rey-Sanchez, A. C., Matheny, A. M., & Mitsch, W. J. (2017). Combining Eddy-covariance and chamber measurements to determine the methane budget from a small, heterogeneous urban floodplain Wetland Park. *Agricultural and Forest Meteorology*, *237–238*, 160–170.

Neubauer, S. C., & Patrick Megonigal, J. (2015). Moving beyond global warming potentials to quantify the climatic role of ecosystems. *Ecosystems*, *18*(6), 1000–1013.

Nisbet, E. G., Manning, M. R., Dlugokencky, E. J., Fisher, R. E., Lowry, D., Michel, S. E., Myhre, C. L., Platt, S. M., Allen, G., Bousquet, P., & Brownlow, R. (2019). Very strong atmospheric methane growth in the 4 years 2014–2017: Implications for the Paris agreement. *Global Biogeochemical Cycles*, *33*, 318–342. https://doi.org/10.1029/2018gb006009

Peng, S., Lin, X., Thompson, R. L., Xi, Y., Liu, G., Hauglustaine, D., Lan, X., Poulter, B., Ramonet, M., Saunois, M., Yin, Y., Zhang, Z., Zheng, B., & Ciais, P. (2022). Wetland emission and atmospheric sink changes explain methane growth in 2020. *Nature*, *612*, 477–482.

Poulter, B., Bousquet, P., Canadell, J. G., Ciais, P., Peregon, A., Saunois, M., Arora, V. K., Beerling, D. J., Brovkin, V., Jones, C. D., Joos, F., Gedney, N., Ito, A., Kleinen, T., Koven, C. D., McDonald, K., Melton, J. R., Peng, C., Peng, S., … Zhu, Q. (2017). Global wetland contribution to 2000–2012 atmospheric methane growth rate dynamics. *Environmental Research Letters*, *12*(9), 094013.

Rey-Sanchez, C., Arias-Ortiz, A., Kasak, K., Chu, H., Szutu, D., Verfaillie, J., & Baldocchi, D. (2022). Detecting hot spots of methane flux using footprint-weighted flux maps. *Journal of Geophysical Research: Biogeosciences*, *127*, e2022JG006977. https://doi.org/10.1029/2022JG006977

Riley, W. J., Subin, Z. M., Lawrence, D. M., Swenson, S. C., Torn, M. S., Meng, L., Mahowald, N. M., & Hess, P. (2011). Barriers to predicting changes in global terrestrial methane fluxes: Analyses using CLM4Me, a methane biogeochemistry model integrated in CESM. *Biogeosciences*, *8*, 1925–1953.

Rinne, J., Tuittila, E. S., Peltola, O., Li, X., Raivonen, M., Alekseychik, P., Haapanala, S., Pihlatie, M., Aurela, M., Mammarella, I., & Vesala, T. (2018). Temporal variation of ecosystem scale methane emission from a boreal fen in relation to temperature, water table position, and carbon dioxide fluxes. *Global Biogeochemical Cycles*, *32*(7), 1087–1106.

Saunois, M., Jackson, R. B., Bousquet, P., Poulter, B., & Canadell, J. G. (2016). The growing role of methane in anthropogenic climate change. *Environmental Research Letters*, *11*(12), 120207.

Saunois, M., Bousquet, P., Poulter, B., Peregon, A., Ciais, P., Canadell, J. G., Dlugokencky, E. J., Etiope, G., Bastviken, D., Houweling, S., Janssens-Maenhout, G., Tubiello, F. N., Castaldi, S., Jackson, R. B., Alexe, M., Arora, V. K., Beerling, D. J., Bergamaschi, P., Blake, D. R., … Zhu, Q. (2016). The global methane budget 2000–2012. *Earth System Science Data*, *8*(2), 697–751.

Saunois, M., Stavert, A. R., Poulter, B., Bousquet, P., Canadell, J. G., Jackson, R. B., Raymond, P. A., Dlugokencky, E. J., Houweling, S., Patra, P. K., Ciais, P., Arora, V. K., Bastviken, D., Bergamaschi, P., Blake, D. R., Brailsford, G., Bruhwiler, L., Carlson, K. M., Carrol, M., … Zhuang, Q. (2020). The global methane budget 2000–2017. *Earth System Science Data*, *12*(3), 1561–1623.

Seiler, C., Melton, J. R., Arora, V. K., & Wang, L. (2021). CLASSIC v1.0: The open-source community successor to the Canadian land surface scheme (CLASS) and the Canadian terrestrial ecosystem model (CTEM)—Part 2: Global benchmarking. *Geoscientific Model Development*, *14*, 2371–2417. https://doi.org/10.5194/gmd-14-2371-2021

Stavert, A. R., Saunois, M., Canadell, J. G., Poulter, B., Jackson, R. B., Regnier, P., Lauerwald, R., Raymond, P. A., Allen, G. H., Patra, P. K., Bergamaschi, P., Bousquet, P., Chandra, N., Ciais, P., Gustafson, A.,

Ishizawa, M., Ito, A., Kleinen, T., Maksyutov, S., … Zhuang, Q. (2022). Regional trends and drivers of the global methane budget. *Global Change Biology*, *28*(1), 182–200.

Wania, R., Melton, J. R., Hodson, E. L., Poulter, B., Ringeval, B., Spahni, R., Bohn, T., Avis, C. A., Chen, G., Eliseev, A. V., Hopcroft, P. O., Riley, W. J., Subin, Z. M., Tian, H., van Bodegom, P. M., Kleinen, T., Yu, Z. C., Singarayer, J. S., Zürcher, S., … Kaplan, J. O. (2013). Present state of global wetland extent and wetland methane modelling: Methodology of a model inter-comparison project (WETCHIMP). *Geoscientific Model Development*, *6*(3), 617–641.

Willard, J., Jia, X., Xu, S., Steinbach, M., & Kumar, V. (2020). Integrating scientific knowledge with machine learning for engineering and environmental systems. arXiv [Physics.Comp-Ph]. arXiv. http://arxiv.org/abs/2003.04919

Yuan, K., Zhu, Q., Li, F., Riley, W. J., Torn, M., Chu, H., McNicol, G., Chen, M., Knox, S., Delwiche, K., Wu, H., Baldocchi, D., Ma, H., Desai, A. R., Chen, J., Sachs, T., Ueyama, M., Sonnentag, O., Helbig, M., … Jackson, R. (2022). Causality guided machine learning model on wetland CH_4 emissions across global wetlands. *Agricultural and Forest Meteorology*, *324*(September), 109115.

Zender, C. S. (2008). Analysis of self-describing gridded geoscience data with netCDF operators (NCO). *Environmental Modelling & Software*, *23*(10), 1338–1342.

Zhang, Z., Fluet-Chouinard, E., Jensen, K., McDonald, K., Hugelius, G., Gumbricht, T., Carroll, M., Prigent, C., Bartsch, A., & Poulter, B. (2021). Development of the global dataset of wetland area and dynamics for methane modeling (WAD2M). *Earth System Science Data*, *13*(5), 2001–2023.

DATA SOURCES

Anthony Bloom, A., Kevin Bowman, W., Lee, M., Alexander Turner, J., Ronny, S., John Worden, R., Richard, W., Kyle McDonald, C., & Daniel Jacob, J. (2017). A global wetland methane emissions and uncertainty dataset for atmospheric chemical transport models (WetCHARTs version 1.0). *Geoscientific Model Development*, *10*(6), 2141–2156.

Arora, V. K., Melton, J. R., & Plummer, D. (2018). An assessment of natural methane fluxes simulated by the CLASS-CTEM model. *Biogeosciences*, *15*(15), 4683–4709.

Bergamaschi, P., Houweling, S., Segers, A., Krol, M., Frankenberg, C., Scheepmaker, R. A., Dlugokencky, E., Wofsy, S. C., Kort, E. A., Sweeney, C., & Schuck, T. (2013). Atmospheric CH_4 in the first decade of the 21st century: Inverse modeling analysis using SCIAMACHY satellite retrievals and NOAA surface measurements. *Journal of Geophysical Research*, *118*(13), 7350–7369.

Bergamaschi, P., Krol, M., Meirink, J. F., Dentener, F., Segers, A., van Aardenne, J., Monni, S., Vermeulen, A. T., Schmidt, M., Ramonet, M., & Yver, C. (2010). Inverse modeling of European CH_4 emissions 2001–2006. *Journal of Geophysical Research*, *115*(D22). https://doi.org/10.1029/2010jd014180

Chandra, N., Patra, P. K., Bisht, J. S., Ito, A., Umezawa, T., Saigusa, N., Morimoto, S., Aoki, S., Janssens-Maenhout, G., Fujita, R., & Takigawa, M. (2021). Emissions from the oil and gas sectors, coal mining and ruminant farming drive methane growth over the past three decades. *Journal of the Asiatic Society of Bangladesh. Humanities*. https://www.jstage.jst.go.jp/article/jmsj/99/2/99_2021-015/_article/-char/ja/

Hayman, G. D., O'Connor, F. M., Dalvi, M., Clark, D. B., Gedney, N., Huntingford, C., Prigent, C., Buchwitz, M., Schneising, O., Burrows, J. P., & Wilson, C. (2014). Comparison of the HadGEM2 climate-chemistry model against in situ and SCIAMACHY atmospheric methane data. *Atmospheric Chemistry and Physics*, *14*(23), 13257–13280.

Ishizawa, M., Mabuchi, K., Shirai, T., Inoue, M., Morino, I., Uchino, O., Yoshida, Y., Belikov, D., & Maksyutov, S. (2016). Inter-annual variability of summertime CO_2 exchange in northern eurasia inferred from GOSAT XCO_2. *Environmental Research Letters*, *11*(10), 105001.

Ito, A., & Inatomi, M. (2012). Use of a process-based model for assessing the methane budgets of global terrestrial ecosystems and evaluation of uncertainty. *Biogeosciences*, *9*(2), 759–773.

Kleinen, T., Brovkin, V., & Schuldt, R. J. (2012). A dynamic model of wetland extent and peat accumulation: Results for the holocene. *Biogeosciences*, *9*(1), 235–248.

Kleinen, T., Mikolajewicz, U., & Brovkin, V. (2020). Terrestrial methane emissions from the last glacial maximum to the preindustrial period. *Climate of the Past*, *16*(2), 575–595.

Maksyutov, S., Oda, T., Saito, M., Janardanan, R., Belikov, D., Kaiser, J. W., Zhuravlev, R., Ganshin, A., Valsala, V. K., Andrews, A., & Chmura, L. (2021). Technical note: A high-resolution inverse modelling technique for estimating surface CO_2 fluxes based on the NIES-TM-FLEXPART coupled transport model and its adjoint. *Atmospheric Chemistry and Physics*. https://doi.org/10.5194/acp-21-1245-2021

McGuire, A. D., Christensen, T. R., Hayes, D., Heroult, A., Euskirchen, E., Yi, Y., Kimball, J. S., Koven, C., Lafleur, P., Miller, P. A., Oechel, W., & Peylin, P. (2012). An assessment of the carbon balance of arctic tundra: Comparisons among observations, process models, and atmospheric inversions. *Biogeosciences Discussions*, *9*(4), 4543–4594.

McNorton, J., Gloor, E., Wilson, C., Hayman, G. D., Gedney, N., Comyn-Platt, E., Marthews, T., Parker, R. J., Boesch, H., & Chipperfield, M. P. (2016). Role of regional wetland emissions in atmospheric methane variability. *Geophysical Research Letters*, *43*(21). https://doi.org/10.1002/2016gl070649

McNorton, J., Wilson, C., Gloor, M., Parker, R. J., Boesch, H., Feng, W., Hossaini, R., & Chipperfield, M. P. (2018). Attribution of recent increases in atmospheric methane through 3-D inverse modelling. *Atmospheric Chemistry and Physics*, *18*(24), 18149–18168.

Melton, J. R., & Arora, V. K. (2016). Competition between plant functional types in the Canadian Terrestrial Ecosystem Model (CTEM) v. 2.0. *Geoscientific Model Development*, *9*(1), 323–361.

Niwa, Y., Fujii, Y., Sawa, Y., Iida, Y., Ito, A., Satoh, M., Imasu, R., Tsuboi, K., Matsueda, H., & Saigusa, N. (2017). A 4D-Var Inversion system based on the icosahedral grid model (NICAM-TM 4D-Var v1.0)—Part 2: Optimization scheme and identical twin experiment of atmospheric CO2 inversion. *Geoscientific Model Development*. https://doi.org/10.5194/gmd-10-2201-2017

Niwa, Y., Tomita, H., Satoh, M., Imasu, R., Sawa, Y., Tsuboi, K., Matsueda, H., Machida, T., Sasakawa, M., Belan, B., & Saigusa, N. (2017). A 4D-Var inversion system based on the icosahedral grid model (NICAM-TM 4D-Var v1.0)—Part 1: Offline forward and adjoint transport models. *Geoscientific Model Development*. https://doi.org/10.5194/gmd-10-1157-2017

Pandey, S., Houweling, S., Krol, M., Aben, I., Chevallier, F., Dlugokencky, E. J., Gatti, L. V., Gloor, E., Miller, J. B., Detmers, R., & Machida, T. (2016). Inverse modeling of GOSAT-retrieved ratios of total column CH4 and CO2 for 2009 and 2010. *Atmospheric Chemistry and Physics*. https://doi.org/10.5194/acp-16-5043-2016

Pasut, C., Tang, F. H., Hamilton, D., Riley, W. J., & Maggi, F. (2021). Spatiotemporal assessment of GHG emissions and nutrient sequestration linked to agro-nutrient runoff in global wetlands. *Global Biogeochemical Cycles*, *35*(4), e2020GB006816.

Patra, P. K., Saeki, T., Dlugokencky, E. J., Ishijima, K., Umezawa, T., Ito, A., Aoki, S., Morimoto, S., Kort, E. A., Crotwell, A., & Kumar, K. R. (2016). Regional methane emission estimation based on observed atmospheric concentrations (2002–2012). 気象集誌. 第2輯, *94*(1), 91–113.

Poulter, B., Bousquet, P., Canadell, J. G., Ciais, P., Peregon, A., Saunois, M., Arora, V. K., Beerling, D. J., Brovkin, V., Jones, C. D., & Joos, F. (2017). Global wetland contribution to 2000–2012 atmospheric methane growth rate dynamics. *Environmental Research Letters*, *12*(9), 094013.

Riley, W. J., Subin, Z. M., Lawrence, D. M., Swenson, S. C., Torn, M. S., Meng, L., Mahowald, N. M., & Hess, P. (2011). Barriers to predicting changes in global terrestrial methane fluxes: Analyses using CLM4Me, a methane biogeochemistry model integrated in CESM. *Biogeosciences*, *8*, 1925–1953.

Ringeval, B., Friedlingstein, P., Koven, C., Ciais, P., de Noblet-Ducoudré, N., Decharme, B., & Cadule, P. (2011). Climate-CH_4 feedback from wetlands and Its interaction with the climate-CO_2 feedback. *Biogeosciences*, *8*(8), 2137–2157.

Spahni, R., Wania, R., Neef, L., van Weele, M., Pison, I., Bousquet, P., Frankenberg, C., Foster, P. N., Joos, F., Prentice, I. C., & Van Velthoven, P. (2011). Constraining global methane emissions and uptake by ecosystems. *Biogeosciences*, *8*(6), 1643–1665.

Tian, H., Chen, G., Lu, C., Xu, X., Ren, W., Zhang, B., Banger, K., Tao, B., Pan, S., Liu, M., & Zhang, C. (2015). Global methane and nitrous oxide emissions from terrestrial ecosystems due to multiple environmental changes. *Ecosystem Health and Sustainability*, *1*(1), 1–20.

Tian, H., Xu, X., Liu, M., Ren, W., Zhang, C., Chen, G., & Lu, C. (2010). Spatial and temporal patterns of CH_4 and N_2O fluxes in terrestrial ecosystems of North America during 1979–2008: Application of a global biogeochemistry model. *Biogeosciences*, *7*(9), 2673–2694.

Tsuruta, A., Aalto, T., Backman, L., Hakkarainen, J., van der Laan-Luijkx, I. T., Krol, M. C., Spahni, R., Houweling, S., Laine, M., Dlugokencky, E., & Gomez-Pelaez, A. J. (2017). Global methane emission estimates for 2000–2012 from carbon-tracker Europe-CH_4 v1.0. *Geoscientific Model Development*, *10*, 1261–1289.

Wang, F., Maksyutov, S., Tsuruta, A., Janardanan, R., Ito, A., Sasakawa, M., Machida, T., Morino, I., Yoshida, Y., Kaiser, J. W., & Janssens-Maenhout, G. (2019). Methane emission estimates by the global high-resolution inverse model using national inventories. *Remote Sensing*, *11*(21), 2489.

Yin, Y., Chevallier, F., Ciais, P., Broquet, G., Fortems-Cheiney, A., Pison, I., & Saunois, M. (2015). Decadal trends in global CO emissions as seen by MOPITT. *Atmospheric Chemistry and Physics*, *15*(23), 13433–13451.

Zhang, Z., Zimmermann, N. E., Kaplan, J. O., & Poulter, B. (2016). Modeling spatiotemporal dynamics of global wetlands: Comprehensive evaluation of a new sub-grid TOPMODEL parameterization and uncertainties. *Biogeosciences*, *13*(5), 1387–1408.

Zheng, B., Chevallier, F., Ciais, P., Yin, Y., Deeter, M. N., Worden, H. M., Wang, Y., Zhang, Q., & He, K. (2018). Rapid decline in carbon monoxide emissions and export from east Asia between years 2005 and 2016. *Environmental Research Letters*, *13*(4), 044007.

Zheng, B., Chevallier, F., Ciais, P., Yin, Y., & Wang, Y. (2018). On the role of the flaming to smoldering transition in the seasonal cycle of African fire emissions. *Geophysical Research Letters*, *45*(21), 11998–12007.

Zhuang, Q., Melillo, J. M., Kicklighter, D. W., Prinn, R. G., McGuire, A. D., Steudler, P. A., Felzer, B. S., & Hu, S. (2004). Methane fluxes between terrestrial ecosystems and the atmosphere at northern high latitudes during the past century: A retrospective analysis with a process-based biogeochemistry model. *Global Biogeochemical Cycles*, *18*(3). https://doi.org/10.1029/2004gb002239

Zhu, Q., Peng, C., Chen, H., Fang, X., Liu, J., Jiang, H., Yang, Y., & Yang, G. (2015). Estimating global natural wetland methane emissions using process modelling: Spatio-temporal patterns and contributions to atmospheric methane fluctuations. *Global Ecology and Biogeography: A Journal of Macroecology*, *24*(8), 959–972.

Zhu, Q., Liu, J., Peng, C., Chen, H., Fang, X., Jiang, H., Yang, G., Zhu, D., Wang, W., & Zhou, X. (2014). Modelling methane emissions from natural wetlands by development and application of the TRIPLEX-GHG model. *Geoscientific Model Development*, *7*(3), 981–999.

SUPPORTING INFORMATION

Additional supporting information can be found online in the Supporting Information section at the end of this article.

How to cite this article: Chang, K.-Y., Riley, W. J., Collier, N., McNicol, G., Fluet-Chouinard, E., Knox, S. H., Delwiche, K. B., Jackson, R. B., Poulter, B., Saunois, M., Chandra, N., Gedney, N., Ishizawa, M., Ito, A., Joos, F., Kleinen, T., Maggi, F., McNorton, J., Melton, J. R. … Zhuang, Q. (2023). Observational constraints reduce model spread but not uncertainty in global wetland methane emission estimates. *Global Change Biology*, *29*, 4298–4312. https://doi.org/10.1111/gcb.16755